

Correspondence

On the Capacity Loss Due to Separation of Detection and Decoding

Ralf R. Müller, *Member, IEEE*, and
Wolfgang H. Gerstaecker, *Member, IEEE*

Abstract—The performance loss due to separation of detection and decoding on the binary-input additive white Gaussian noise (AWGN) channel is quantified in terms of mutual information. Results are reported for both the code-division multiple-access (CDMA) channel in the large system limit and the intersymbol interference (ISI) channel. The results for CDMA rely on the replica method developed in statistical mechanics. It is shown that a previous result of Shamai and Verdú found for Gaussian input alphabet holds also for binary input alphabets. For the ISI channel, the performance loss is calculated via the Bahl–Cocke–Jelinek–Raviv (BCJR) algorithm. Comparisons are made to the capacity of separate detection and decoding using suboptimum detectors such as a decision-feedback equalizer.

Index Terms—Channel capacity, code-division multiple access (CDMA), fading channels, intersymbol interference (ISI), maximum a posteriori (MAP) detection, replica method, statistical mechanics.

I. INTRODUCTION

Separation of detection and decoding, though suboptimum in general, is widespread in communications technology. This is due to the huge complexity which is required by the optimum joint approach. Examples are Global System for Mobile Communications (GSM) [2] where a soft-output Viterbi equalizer (Bahl–Cocke–Jelinek–Raviv (BCJR) algorithm [3]) is used for detection first and then another Viterbi algorithm is used for decoding, xDSL (digital subscriber lines), where separate decision-feedback equalization (e.g., implemented with equivalent precoding) or reduced-state equalization is performed before channel decoding, and Universal Mobile Telecommunications System (UMTS), where state-of-the-art receivers rely on separate detection using a Rake receiver and turbo decoding.

While separate processing is used frequently, little is known about its loss in terms of channel capacity compared to optimum joint processing. In this correspondence, that loss is investigated for binary transmission. In Section II, we derive a general formula for the capacity of separate processing. This formula is specialized to code-division multiple access (CDMA) with random signature sequences in the large system limit in Section III, exploiting results by Tanaka [4] which have been obtained using concepts from statistical mechanics. In Section IV, the BCJR algorithm [3] is used to evaluate the loss of separate processing for intersymbol interference (ISI) channels, and comparisons to separate processing with suboptimum detection are made. Numerical examples are given for both cases. A short summary and conclusions are given in Section V.

Manuscript received April 4, 2002; revised October 14, 2003. The material in this correspondence was presented in part at the IEEE International Symposium on Advances in Wireless Communications, Victoria, BC, Canada, September 2002 and the IEEE Information Theory Workshop, Bangalore, India, October 2002.

R. R. Müller is with the Forschungszentrum Telekommunikation Wien (ftw), Tech Gate Vienna, 1220 Vienna, Austria (e-mail: mueller@ftw.at).

W. H. Gerstaecker is with the Telecommunications Laboratory, University of Erlangen-Nuremberg, 91058 Erlangen, Germany (e-mail: gersta@Int.de).

Communicated by A. Kavčić, Associate Editor for Detection and Estimation. Digital Object Identifier 10.1109/TIT.2004.831854

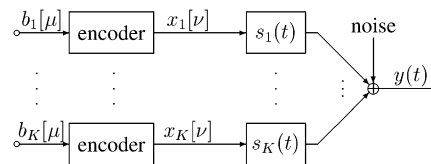


Fig. 1. Gaussian multiple-access channel with K users.

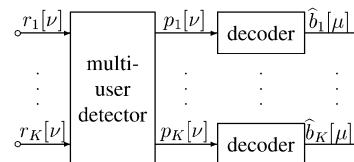


Fig. 2. Separation of multiuser detection and decoding.

II. EQUIVALENT BINARY-SYMMETRIC CHANNEL

Consider a synchronous, memoryless Gaussian multiple-access channel with correlated waveforms and K users, as depicted in Fig. 1. It is well known [5] that the appropriately sampled output of a filter bank matched to the K waveforms $s_k(t)$, $1 \leq k \leq K$, is a sufficient discrete-time statistics $\mathbf{r}[\nu]$ for the signal $y(t)$. As long as the users' individual information rates lie within the capacity region of the channel there is a coding scheme that enables perfect reconstruction of the transmitted information $b_k[\mu]$, $1 \leq k \leq K$, from the knowledge of the vector series $\mathbf{r}[\nu]$.

With respect to the data processing lemma, it is not obvious whether this reconstruction can be handled by the structure in Fig. 2. Hereby, the "multiuser detector" is allowed to be any algorithm that has no knowledge about the code laws while the independent decoders are assumed to have no knowledge about the users' waveforms.

Without loss of generality, consider now the single-user channel from x_1 to p_1 . Assume that the multiuser detector does its job in an individually optimum fashion. Thus, its output is canonically given by the *a posteriori* probability (APP)

$$p_1 = \Pr(x_1 = 1 | \mathbf{r}). \quad (1)$$

Note that this is also the canonical output of an optimum soft-output equalizer for an ISI channel.

For the further development of the correspondence, the following lemma (proven in Appendix I) will be essential.

Lemma 1: Consider an arbitrary memoryless channel with binary input X and output $Y \in \mathcal{Y}$. Let $P_e(y)$ denote the minimum uncoded probability of detection error of this channel conditioned on the observation of the output symbol $Y = y$. Then, the mutual information is given by

$$I(X; Y) = H(X) - \mathbb{E}_y \mathcal{H}(P_e(y)) \text{ [bit]} \quad (2)$$

with the binary entropy function

$$\mathcal{H}(x) \triangleq -x \log_2(x) - (1-x) \log_2(1-x). \quad (3)$$

A similar result has been obtained in [6] for the capacity of a binary-input symmetric-output memoryless channel. Such a channel is defined via

$$p(Y = y | X = 1) = p(Y = -y | X = -1) \quad (4)$$

($p(Y|X)$: transition probability (density)) and is a special case of the channel considered in Lemma 1. According to [6, eq. (4.1)] the capacity of this channel is

$$C = 1 - \mathbb{E}_y [\log_2(1 + e^{-u}) | X = 1] \quad (5)$$

with the log-likelihood ratio (LLR)

$$u = \ln \frac{p(y | X = 1)}{p(y | X = -1)} \quad (6)$$

which depends on the channel output and the transition probability. Using straightforward calculations, (5) can be transformed to (2) with $H(X) = 1$.

The capacity of separated detection and decoding is defined as the maximum mutual information between the input X_1 and the random variable P_1 corresponding to the APP of (1)

$$C_{\text{sep}} \triangleq \max_{P_1(X_1)} I(X_1; P_1). \quad (7)$$

If we now constrain to channels whose capacity is achieved by equiprobable inputs, e.g., symmetric channels, Lemma 1 yields for the capacity of separated detection and decoding

$$C_{\text{sep}} = 1 - \mathbb{E}_{p_1} \mathcal{H}(P_e(p_1)). \quad (8)$$

Note that this is the capacity of a binary-symmetric channel where the crossover probability is varying and the channel state is known to the receiver only.

Since p_1 is a deterministic function of \mathbf{r} , see (1), averaging over p_1 is equivalent to averaging over \mathbf{r} . This yields

$$C_{\text{sep}} = 1 - \mathbb{E}_{\mathbf{r}} \mathcal{H}(P_e(p_1)) \quad (9)$$

$$= 1 - \mathbb{E}_{\mathbf{r}} \mathcal{H}(p_1). \quad (10)$$

Note that (9) is the capacity for "soft" detection. The capacity for hard detection is smaller and reads

$$C_{\text{sep}}^{\text{hard}} = I\left(X_1; \text{sign}\left(P_1 - \frac{1}{2}\right)\right) = 1 - \mathcal{H}\left(\mathbb{E}_{\mathbf{r}} P_e(p_1)\right). \quad (11)$$

Equations (9) and (11) show that the loss due to hard detection is exactly the loss incurred by averaging the argument of the convex function $-\mathcal{H}(\cdot)$ instead of averaging the convex function itself.

III. RANDOM CDMA

For CDMA with random signature sequences, the expectation in (9) can be evaluated by computer simulations as in [7]. For asymptotically large systems—number of users and spreading gain growing with fixed ratio toward infinity—analytical results can be obtained using a tool from statistical mechanics which is called *replica method* [8]. Though its rigorous mathematical justification is still an open problem which by far exceeds the scope of this work, it has been shown to give sensible results in context of multiuser detection by Tanaka [4].

Proposition 1 (Tanaka): Let the symbol alphabet be $\{+1; -1\}$, the signature sequences be independent and identically distributed (i.i.d.) Gaussian random variables, and the number of users K and the spreading factor N grow to infinity, but the load $\beta = K/N$ remain fixed. Moreover, assume that the replica method may be applied¹ and the capacity for joint decoding converges to a nonrandom limit. Then, in the presence of additive white Gaussian noise (AWGN) of variance

¹See [4], [9] for further details about this condition.

σ^2 , the multiuser efficiency η (see [10] for definition) is a solution to the fixed point equation

$$\frac{1}{\eta} = 1 + \frac{\beta}{\sigma^2} \left[1 - \sqrt{\frac{\eta}{2\pi\sigma^2}} \int_{\mathbb{R}} \tanh\left(\frac{\eta}{\sigma^2}x\right) \times \exp\left(-\frac{\eta(x-1)^2}{2\sigma^2}\right) dx \right] \quad (12)$$

and the capacity for joint decoding in nats is given in terms of the multiuser efficiency as

$$C_{\text{joint}}(\eta) = \frac{\eta}{\sigma^2} + \frac{\eta - 1 - \log \eta}{2\beta} - \sqrt{\frac{\eta}{2\pi\sigma^2}} \times \int_{\mathbb{R}} \log \left[\cosh\left(\frac{\eta}{\sigma^2}x\right) \right] \exp\left(-\frac{\eta(x-1)^2}{2\sigma^2}\right) dx. \quad (13)$$

In case (12) has multiple solutions, the correct one is that solution for which $C_{\text{joint}}(\eta)$ is smallest.

Note that Proposition 1 does not state the convergence of the capacity for joint decoding, but assumes it. This assumption is plausible, since the convergence for Gaussian input signals is proven [11]. Recently, Tanaka's result was generalized by Guo and Verdú [12] to arbitrary power distributions among the users. In order to keep notation simple and to concentrate on the essential ideas, we do not consider users with different power levels in this correspondence, since the generalization of the results of this section to any power distribution is straightforward given the results available in [12].

Proposition 2: Consider the same conditions as in Proposition 1. Then, the capacity for separated detection and decoding in nats is given in terms of the multiuser efficiency (12) as

$$C_{\text{sep}}(\eta) = \frac{\eta}{\sigma^2} - \sqrt{\frac{\eta}{2\pi\sigma^2}} \times \int_{\mathbb{R}} \log \left[\cosh\left(\frac{\eta}{\sigma^2}x\right) \right] \exp\left(-\frac{\eta(x-1)^2}{2\sigma^2}\right) dx. \quad (14)$$

This proposition is proven in various ways in Appendixes II–IV. Though a single proof would be sufficient to state Proposition 2, each proof gives different intuitive insight into why the proposition holds. The first proof makes use of Lemma 1 and uses a result from [4] on the moments of analytic functions of the error probability. The second proof starts from the chain rule of mutual information and ends up plugging (12) into the derivative of (13) with respect to η . The third proof requires the additional assumption that the self-averaging property with respect to the signature sequences holds for all moments of the detector output signal and, therefore, is less general. However, it establishes the existence of an equivalent AWGN channel seen at the detector output. Considering the loss due to separation of detection and decoding

$$C_{\text{joint}}(\eta) - C_{\text{sep}}(\eta) = \frac{\eta - 1 - \log \eta}{2\beta} \text{ [nat]} \quad (15)$$

we find a striking analogy to Theorem IV.1 in [1] which states the same loss due to separation of detection and decoding for Gaussian² instead of binary inputs. Moreover, Müller [13] conjectured that (15) holds regardless of the input distribution and, in very recent work, Guo and Verdú [14], [15] have proven him right.

The third proof of Proposition 2 in Appendix IV shows that (14) is the capacity for separate detection and decoding whenever there is an

²Note that due to different normalizations (spectral efficiency on complex-valued channel versus per-user capacity on real-valued channel), the term 2β in the denominator does not occur in [1]. Note also that the linear minimum mean-square error (MMSE) estimate considered in [1] is the maximum *a posteriori* (MAP) estimate for Gaussian inputs.

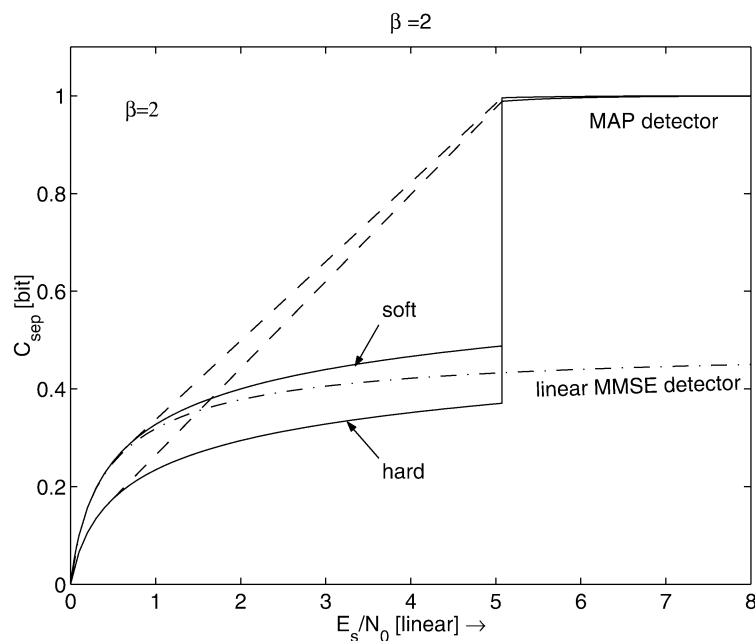


Fig. 3. Capacity over signal-to-noise ratio in linear scale. The dashed line refers to the convex hull. For comparison, the linear MMSE detector is shown by the dash-dotted line.

equivalent AWGN channel which can be parametrized by some multiuser efficiency η . This means, replacing the nonlinear MMSE estimator by a less complex linear MMSE estimator for separated detection and decoding still gives the capacity stated in (14), but with the multiuser efficiency being defined by the well-known Tse–Hanly [16] equation

$$\frac{1}{\eta_{\text{LMMSE}}} = 1 + \frac{\beta}{\sigma^2 + \eta_{\text{LMMSE}}}. \quad (16)$$

This is, since for the linear MMSE detector the residual interference at the detector output is known to be Gaussian asymptotically [17], [18].

The capacity of the separated approach can be increased by means of error-free (post decoding) decision feedback combined with successive cancellation. Then, the users experience a virtual load β' which is uniformly distributed within $[0; \beta]$. Thus, capacity under that constraint is given by

$$C_{\text{sep}}^{\text{DFE}}(\eta) = \frac{1}{\beta} \int_0^\beta C_{\text{sep}}(\eta(\beta')) d\beta'. \quad (17)$$

For linear MMSE detection, this yields with (16)

$$C_{\text{sep, LMMSE}}^{\text{DFE}}(\eta) = \frac{1}{\beta} \int_\eta^1 \left(1 + \frac{\sigma^2}{\eta'^2}\right) C_{\text{sep}}(\eta') d\eta'. \quad (18)$$

It is known from [1] that fading can help to increase capacity for separation of detection and decoding if the symbol alphabet is Gaussian. However, this effect is due to shaping the interference in a more favorable way. If the fading process is identical to all users, fading is a destructive effect for Gaussian symbol alphabet. Surprisingly, this is different for binary alphabet. This is illustrated in Fig. 3, where capacity is plotted versus the signal-to-noise ratio in *linear* scale. Obviously, capacity is a nonconcave function of the signal-to-noise ratio. Thus, a higher capacity can be achieved by modulating the signal power in an appropriate way. If we constrain the assigned powers to be identical for each user, but variable over time, one can achieve the rate which corresponds to the convex hull of the rate for constant power. The points on the convex hull can be obtained by switching the power between

the two signal-to-noise ratio points where the convex hull touches the curve for constant power. The relative period of time for which the one or the other power level is used determines the time-averaged power and therefore which point on the convex hull is achieved. Interchanging powers with rates, this scheduling is equivalent to achieving a rate point on the dominant face of the capacity region of a two-user multiple-access channel by time sharing between the vertices.

It is also remarkable to observe from Fig. 3 that without power scheduling, channel capacity is not a continuous function of the signal-to-noise ratio. Such effects are well known in statistical mechanics and called phase transitions [8]. The phase transition in Fig. 3 occurs, as the multiuser efficiency (12) undergoes a phase transition for the considered load as the signal-to-noise ratio increases, cf. [4, Fig. 4]. The discontinuity of multiuser efficiency means that there is a waterfall region in the bit-error rate. Via Lemma 1, the jump in bit-error rate translates into a jump in capacity.

Considering hard detection obviously incurs some loss. However, this loss appears to be very small on the right side of the phase transition, i.e., for high signal-to-noise ratios.

The loss due to separation of detection and decoding is quantified implicitly via (15) in terms of the multiuser efficiency. For an explicit comparison, it is convenient [11], [19] to characterize the spectral efficiency of the system

$$\Gamma = \beta C \quad (19)$$

as a function of the normalized signal-to-noise ratio

$$\frac{E_b}{N_0} = \frac{E_s}{N_0} / C. \quad (20)$$

This tradeoff between power efficiency and bandwidth efficiency is shown in Fig. 4 for several loads. For overloaded systems, the spectral efficiency of joint decoding is close to the single-user bound, unless it runs into saturation due to the finite alphabet size. Separate decoding severely degrades spectral efficiency for low signal-to-noise ratios. For high signal-to-noise ratios, both systems run into saturation and the loss (15) vanishes due to a well-known result of Tse and Verdú [20]

$$\lim_{\sigma \rightarrow 0} \eta = 1. \quad (21)$$

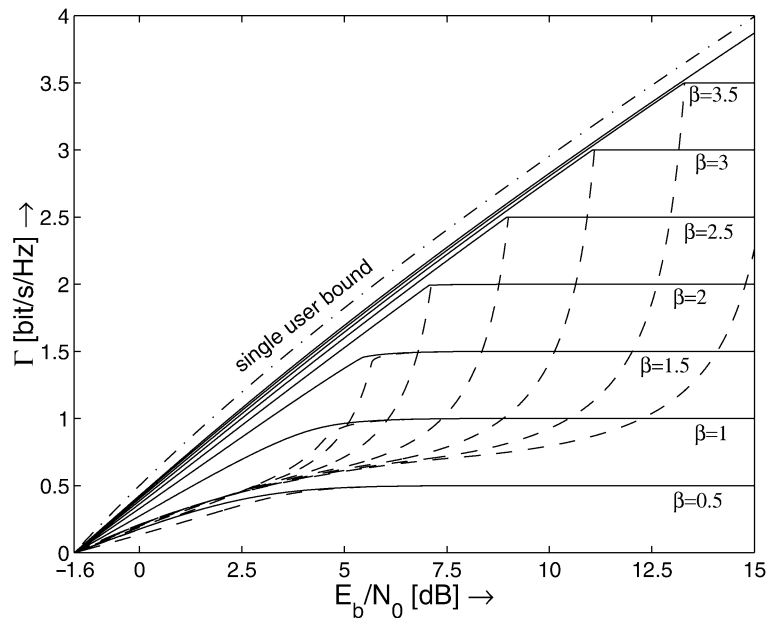


Fig. 4. Spectral efficiency versus normalized signal-to-noise ratio for several loads. Solid and dashed lines refer to the joint and separate (soft detection with power scheduling) decoding approach, respectively.

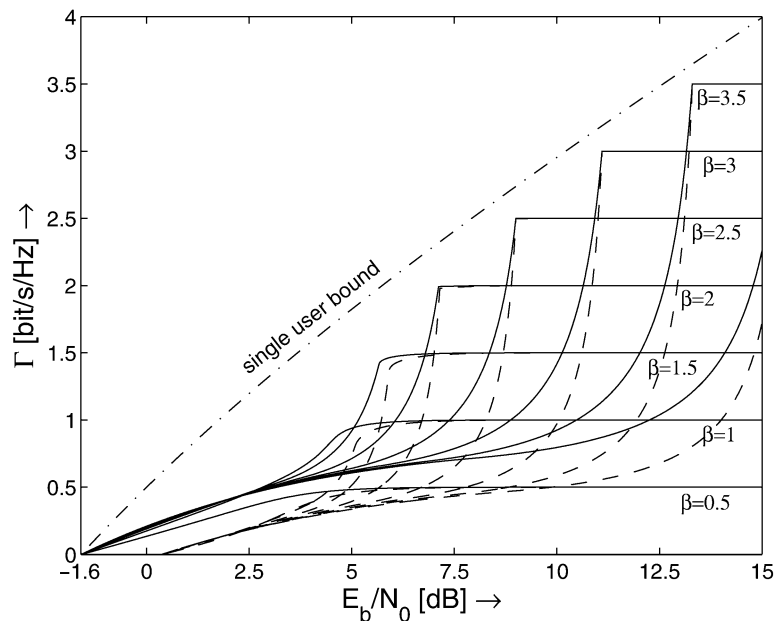


Fig. 5. Spectral efficiency versus normalized signal-to-noise ratio for several loads and separate detection and decoding. Solid and dashed lines refer to soft and hard detection (with power scheduling), respectively.

Separate decoding is only close to the single-user bound for overloaded systems and for a particular signal-to-noise ratio which heavily depends on the load. This makes performance close to the single-user bound possible in principle, but very hard to achieve in practice.

Fig. 5 compares the separated capacities for soft and hard detection. The loss of hard detection is small for large signal-to-noise ratios and asymptotically vanishing due to (21). For vanishing spectral efficiency, a power penalty of $10 \log_{10}(\pi/2) \approx 1.96$ dB appears. This power penalty is well known for hard detection in single-user communications [21]. Simulation results for finite number of users and hard detection can be found in [19, Sec. 4.5.1].

It is also insightful to compare the spectral efficiency of binary signaling to that of Gaussian signaling reported in [11]. Though the gap between the capacities of joint and separate decoding is identical in terms of multiuser efficiency, the actual gap for a given signal-to-noise

ratio behaves very different. An example for soft detection is given in Fig. 6. For joint decoding, Gaussian input alphabet is optimum. The restriction to binary symbols results in a saturation of spectral efficiency at the load. This effect accounts for almost all of the suboptimality of binary signaling with joint decoding. Considering separate detection and decoding, binary signaling wins against Gaussian signaling for loads larger than a certain threshold load near $\beta = 1$. For increasing load, its spectral efficiency follows indistinguishably close its counterpart with joint decoding, until it almost drops down to spectral efficiency of Gaussian inputs at some threshold load where a phase transition of the multiuser efficiency occurs. With power modulation, this drop-down is considerably smoother.

Linear MMSE detection with binary input is severely suboptimum in comparison to MAP detection for medium-range loads. For both large and small loads, its suboptimality vanishes. This is as for $\beta \rightarrow 0$ and

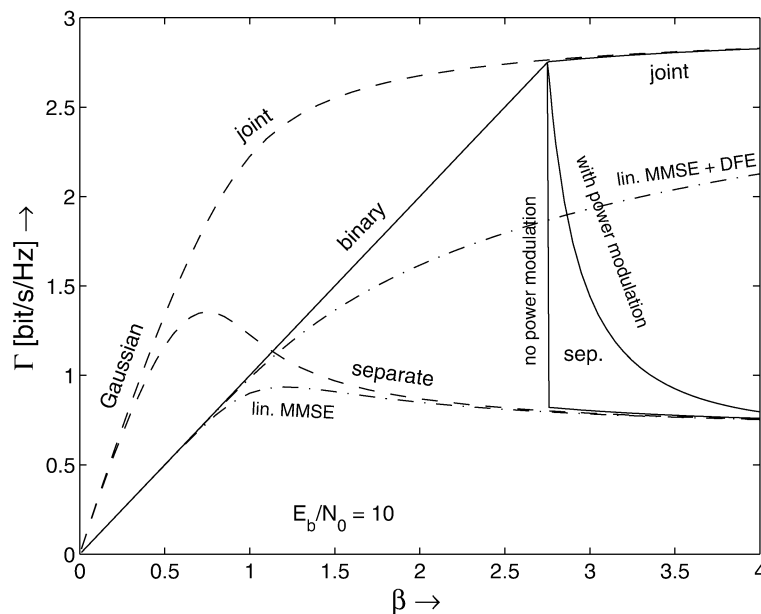


Fig. 6. Spectral efficiency versus load for $E_b/N_0 = 10$ dB, binary (solid lines) versus Gaussian (dashed lines) input alphabet. For comparison, the dash-dotted lines refer to linear MMSE detection with binary input.

$\beta \rightarrow \infty$, the multiuser efficiencies of both the linear MMSE detector and the MAP detector tend toward 1 and 0, respectively. In combination with successive cancellation, linear MMSE detection achieves the joint decoding capacity for Gaussian inputs [22]. This is not true for binary inputs; however, it holds for asymptotically large loads due to (17).

IV. INTERSYMBOL INTERFERENCE

For ISI channels, the optimum approach of joint equalization and decoding using the super trellis diagram is not feasible, in general. Therefore, in most practical applications, equalization and decoding are separated. For example, in the GSM system [2] a BCJR algorithm [3] or a suboptimum approximation thereof [23] is used for calculation of APPs of the transmitted symbols exploiting the entire received signal of a block, and subsequently, a soft-input channel decoder is employed. Because unreliable equalizer outputs often occur in bursts, an interleaver is inserted after channel coding, and deinterleaving is performed at the equalizer output. Hence, the equivalent channel for decoding is a memoryless³ channel with particular known output statistics according to the given APPs, and the results of Section II can be applied in case of binary transmission for evaluation of the capacity of separate soft-output equalization and decoding. According to (8)

$$C_{\text{sep}} = 1 - \mathbb{E}_{\mathbf{r}} \mathcal{H}(\text{APP}[\nu]) \quad (22)$$

where $\text{APP}[\nu]$ denotes the APP of the ν th transmitted symbol⁴ when the entire received signal is known

$$\text{APP}[\nu] \triangleq \Pr(x[\nu] = 1 | \mathbf{r}) \quad (23)$$

with

$$\mathbf{r} \triangleq [r[0], r[1], \dots, r[L-1]] \quad (24)$$

³Ideal interleaving is assumed.

⁴We use equiprobable inputs for convenience, and it turns out that this makes the compound channel symmetric in the sense of Gallager (see [24] for a definition) [25], [6]. For symmetric channels with equiprobable inputs, (22) is valid.

where L denotes the number of transmitted symbols per block. The received signal samples are given by

$$r[\nu] = \sum_{\kappa=0}^{q_h} g[\kappa] x[\nu - \kappa] + n[\nu] \quad (25)$$

with binary antipodal i.i.d. transmit symbols $x[\nu]$, AWGN $n[\nu]$ with variance σ^2 , and the discrete-time DFE channel impulse response $g[\kappa]$ of order q_h .⁵

Hence, according to (22), capacity may be evaluated numerically by calculating APPs via the BCJR algorithm and averaging $1 - \mathcal{H}(\text{APP}[\nu])$ over a sufficiently long burst. This observation has been also made independently by Kavčić *et al.* in [26]. It should be noted that a code with rate higher than C_{sep} for which decoding error probability can be made arbitrarily small cannot be found if the memory in the output of the BCJR algorithm is ignored or, equivalently, perfect interleaving is applied. Otherwise, higher rates might be achieved if the decoder is adjusted to the correlation in the BCJR output sequence, i.e., no converse exists for C_{sep} . Hence, in situations where the interleaver size is not much larger than the codeword length one might refrain from referring to the information rates in (22) as capacity, cf. [26].

Channel capacity for separate optimum soft-output equalization and decoding has been also considered in [25, Sec. III.B], where it has been shown that an information rate according to (5) can be achieved if the memory of the output of the BCJR algorithm is ignored [25, eq. (4)].

Of course, it is interesting to compare C_{sep} to the capacity of optimum joint processing. For (discrete-time) ISI channels with non-Gaussian i.i.d. inputs, no closed-form results are available in general on capacity but only bounds [27]. Recently, a numerical method has been provided in [28], [25], [29]. In this approach, capacity is evaluated numerically exploiting the forward recursion of the BCJR algorithm. Hence, similar to separate equalization and decoding, capacity of joint processing under the restriction to equiprobable i.i.d. inputs can be determined from a run of the BCJR algorithm over a long block. An extension to finite-alphabet Markov input processes is

⁵In this section, single-user transmission is considered. Therefore, the user index k has been omitted.

possible [28], [25], [29]. In [30] and [31], tight lower and upper bounds on unconstrained capacity for optimized Markov input processes are reported.

It is also interesting to consider soft-output decision-feedback equalization (DFE) instead of optimum soft-output equalization and to determine the capacity of DFE along with decoding, making the standard assumption of error-free DFE feedback symbols. In a DFE with soft output, the signal after feedback is passed on to the channel decoder. In the case of a zero-forcing (ZF) DFE, an equivalent binary-input AWGN channel results after equalization⁶ with⁷

$$(E_s/N_0)_{\text{equiv}}^{\text{ZF-DFE}} = |g|^2/(2\sigma^2)$$

and for evaluation of capacity the results of the third proof of Proposition 2 in Appendix IV (capacity of binary-input AWGN channel) can be directly used. If an MMSE-DFE [32] is applied instead of a ZF-DFE, the decoder sees an overall channel with a distortion composed of precursor ISI and noise. Assuming a Gaussian distribution for the distortion and ignoring the memory due to the precursor part corresponding to ideal interleaving, an equivalent AWGN channel with

$$(E_s/N_0)_{\text{equiv}}^{\text{MMSE-DFE}} = \frac{1}{2} \text{SNR}_{\text{MMSE-DFE},u}$$

results, with the MMSE-DFE output signal-to-noise ratio after bias compensation [32]

$$\text{SNR}_{\text{MMSE-DFE},u} = e^T \int_{-1/(2T)}^{1/(2T)} \ln\left(\frac{1}{\sigma^2} |G(e^{j2\pi f T})|^2 + 1\right) df - 1 \quad (26)$$

where T and $G(e^{j2\pi f T})$ denote the symbol interval and the Fourier transform of $g[\cdot]$, respectively. Again, the results of Appendix IV (third proof of Proposition 2) can be directly used for capacity calculation. However, it should be noted that, in general, the Central Limit Theorem is not applicable to the precursor part of the distortion [27], and the Gaussian assumption for the distortion may be violated. Nevertheless, according to a conjecture of Shamai and Laroia [27, Sec. II-F], the MMSE-DFE channel capacity using the Gaussian assumption may serve as a lower bound for the true channel capacity of MMSE-DFE which is obtained from the actual probability density function (pdf) of the distortion. However, a proof for this conjectured lower bound is missing yet.

It is worth mentioning that via Lemma 1, also the capacity of a DFE with erroneous feedback symbols can be calculated, i.e., of a DFE with feedback symbols delivered by a slicer applied to the signal after feedback instead of the decoder. For this, the pdf of the slicer input signal $y[\cdot]$ has to be measured and the (uncoded) symbol error rate corresponding to each value of y (or signal values in sufficiently small intervals). Equipped with these statistics, one can apply Lemma 1 directly.

Finally, we consider soft-output linear equalization (LE) and capacity for separate processing under this restriction to the equalizer. Because ZF-LE is not able to cope with channels with spectral nulls, we restrict ourselves to MMSE-LE. Here, the distortion in the equalizer output consists of precursor and postcursor ISI and noise. According to [17], the Gaussian assumption is approximately valid for the distortion under many conditions. Hence, again an overall AWGN channel may be assumed for decoding with

$$(E_s/N_0)_{\text{equiv}}^{\text{MMSE-LE}} = \frac{1}{2} \text{SNR}_{\text{MMSE-LE},u}$$

⁶Therefore, the interleaving assumption can be dropped.

⁷Here we have assumed that the channel is minimum phase and no feedforward filter is required.

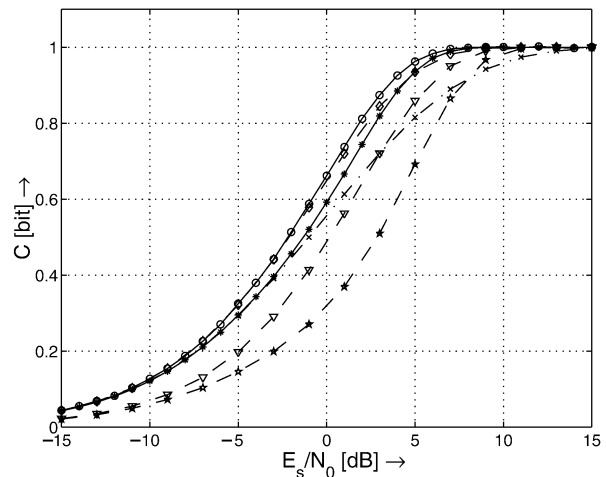


Fig. 7. Capacity of decode channel versus E_s/N_0 for optimum joint processing (solid line, "o"), separate optimum equalization and decoding (solid line, "*"), MMSE-DFE with perfect feedback (dashed line, "◇"), ZF-DFE with perfect feedback (dashed line, "▽"), ZF-DFE with erroneous feedback (dashed line, "*"), and MMSE-LE (dash-dotted line, "x").

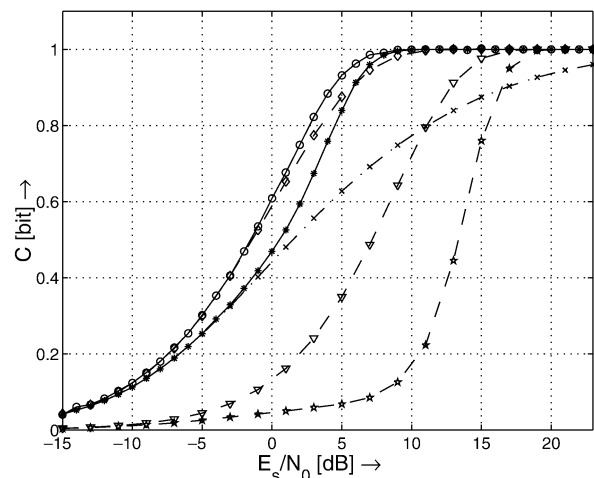


Fig. 8. Capacity of E2PR4 channel versus E_s/N_0 for optimum joint processing (solid line, "o"), separate optimum equalization and decoding (solid line, "*"), MMSE-DFE with perfect feedback (dashed line, "◇"), ZF-DFE with perfect feedback (dashed line, "▽"), ZF-DFE with erroneous feedback (dashed line, "*"), and MMSE-LE (dash-dotted line, "x").

where the signal-to-noise ratio of the unbiased MMSE-LE is given by [33], [32]

$$\text{SNR}_{\text{MMSE-LE},u} = \frac{1}{T \int_{-1/2T}^{1/2T} \frac{1}{\sigma^2 |G(e^{j2\pi f T})|^2 + 1} df} - 1 \quad (27)$$

and is always lower than that of unbiased MMSE-DFE because in (27) the harmonic mean is applied to $\frac{1}{\sigma^2} |G(e^{j2\pi f T})|^2 + 1$ whereas in (26) the geometric mean appears, cf. [34].

In the following, numerical results are shown for the typical magnetic recording channels decode ($q_h = 1$), E2PR4 ($q_h = 4$), and CH6 ($q_h = 6$), whose impulse responses are given, e.g., in [28]. All channels have zeros only on the unit circle. Therefore, the channels are minimum phase, and no feedforward filter is required for the DFE schemes. Figs. 7–9 show C_{joint} (solid lines, "o") for binary equiprobable i.i.d.

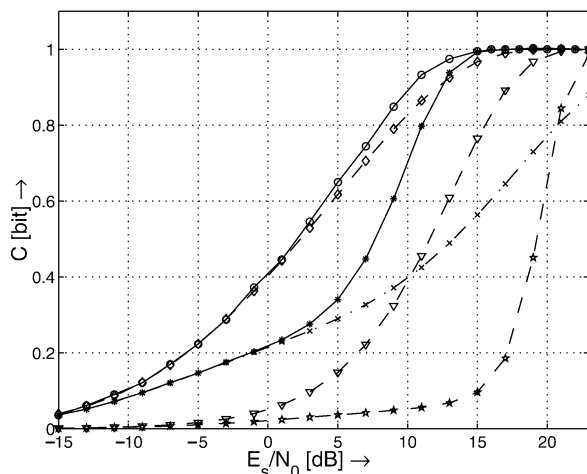


Fig. 9. Capacity of CH6 channel versus E_s/N_0 for optimum joint processing (solid line, “o”), separate optimum equalization and decoding (solid line, “*”), MMSE-DFE with perfect feedback (dashed line, “◇”), ZF-DFE with perfect feedback (dashed line, “▽”), ZF-DFE with erroneous feedback (dashed line, “*”), and MMSE-LE (dash-dotted line, “×”).

inputs⁸ according to [28] and C_{sep} (solid lines, “*”) versus E_s/N_0 for all channels. In principle, the loss due to separation of equalization and channel decoding increases with increasing channel order/channel distortion. The smallest loss results for the dicode channel, whereas the loss is significant for the CH6 channel. Here, a curve similar to those for CDMA with $\beta > 1$ is obtained. Hence, for severely distorting channels, the code rate should be adapted to the separated receiver structure. Furthermore, the significant loss of separate equalization and decoding for severely distorting channels suggests iterative equalization and decoding in order to approach the capacity of joint processing.

Figs. 7–9 show also the capacity of the three considered DFE schemes (dashed lines). MMSE-DFE (“◇”) approaches the capacity of optimum joint processing especially for low-to-moderate signal-to-noise ratios remarkably close, cf. also [27], whereas there is a small gap before both curves run into saturation.⁹ This can be explained from the fact that for low signal-to-noise ratios, binary and Gaussian signaling becomes equivalent and MMSE-DFE is optimum in terms of capacity for Gaussian signals. The capacity of separate optimum equalization and decoding is clearly surpassed because the assumption of perfect feedback symbols implicitly requires some combination of MMSE-DFE and decoding, i.e., already decoded symbols have to be used for feedback. A corresponding realizable scheme which asymptotically achieves the capacity of MMSE-DFE with perfect feedback for any signal-to-noise ratio has been proposed by Guess and Varanasi [35]. Here, postcursor symbols required for feedback belong to different codewords than the considered symbols which are already decoded. This can be guaranteed by proper interleaving/deinterleaving.¹⁰ A similar multistage scheme using an APP detector in each stage has been proposed by Pfister *et al.* in [25]. The

⁸For low signal-to-noise ratios, a noticeably higher information rate than for i.i.d. inputs is achievable with Markov input processes [28], [30], [31]. In this case, the maximum information rate achievable with i.i.d. equiprobable input symbols differs from the capacity and is sometimes called the symmetric information rate (SIR) [25] instead.

⁹For different, less distorting channels both capacities may be in good accordance over the whole range of signal-to-noise ratio, cf. [27].

¹⁰Without interleaving, i.e., if sequence-wise or vector processing is assumed in conjunction with MMSE-DFE, it has been shown for Gaussian signals in [27] that ideal feedback is a fictitious assumption that cannot be realized as it yields a higher capacity than optimum joint processing. On the other hand, considering mutual information on a symbol-by-symbol basis corresponding to ideal interleaving, MMSE-DFE preserves channel capacity in the Gaussian case and is implementable.

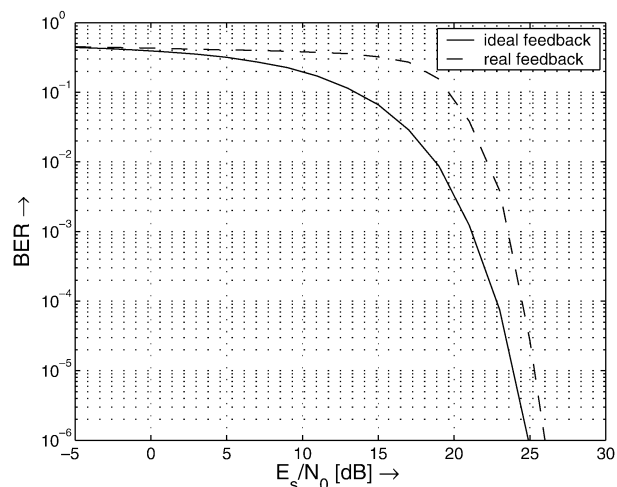


Fig. 10. Bit-error rate of ZF-DFE versus E_s/N_0 for CH6 channel, using correct symbols (solid line) and detected symbols (dashed line) for feedback, respectively.

corresponding information rate also approaches that of optimum joint processing. Furthermore, a nested lattice precoding scheme introduced by Zamir, Shamai, and Erez [36] may be used alternatively for approaching the capacity of MMSE-DFE at any signal-to-noise ratio.¹¹

This is in contrast to previously proposed precoding techniques like Tomlinson–Harashima precoding [37] which are optimum in principle only for high signal-to-noise ratio. Thus, MMSE-DFE is realizable and might be an interesting alternative to iterative equalization and decoding for approaching the capacity of optimum joint processing. However, it should be noted that the schemes in [35], [25], [36] do not separate detection and decoding completely, but are characterized by a multistage nature with alternating equalization and decoding. Hence, the given MMSE-DFE information rates are also only achievable with multistage processing.

Comparing the results for ZF-DFE (“▽”) to those for MMSE-DFE, a significant performance degradation can be observed for low-to-moderate signal-to-noise ratios. Hence, also for binary signaling, the MMSE criterion is essential in this regime. ZF-DFE suffers also a significant loss compared to optimum soft-output equalization. A reason for this might be that the considered channels have zeros only at the unit circle. Among all minimum-phase channels, such channels have the worst energy concentration in the front part of the impulse response since $|g[\kappa]| = |g[q_h - \kappa]|$, $\kappa \in \{0, 1, \dots, q_h\}$ [38], which results in

$$\sum_{\kappa=0}^{\mu} |g[\kappa]|^2 = \sum_{\kappa=q_h-\mu}^{q_h} |g[\kappa]|^2, \quad \mu \in \{0, 1, \dots, q_h\}.$$

A significant portion of the total received energy cannot be used constructively in the DFE detection process because the front part and the back part of the impulse response have the same energy.

Using erroneous symbol-by-symbol decisions of the slicer instead of decoded symbols for feedback in ZF-DFE yields an additional loss of up to 8 dB for the considered examples. The corresponding curves (“*”) have been obtained via Monte Carlo simulations as described above. The high loss can be attributed to the well-known fact that error propagation significantly deteriorates the performance of a DFE for channels with severe ISI and low-to-moderate signal-to-noise ratios, cf. e.g., [39]. This is confirmed by Fig. 10 which shows the bit-error rate of ZF-DFE for the CH6 channel, using ideal feedback and feedback of detected symbols, respectively. For severely distorting channels, in

¹¹For this, the transmitter and receiver have to use a common *dither sequence* (common randomness), i.e., additional side information is required.

general, some kind of waterfall region appears in the bit-error rate of a DFE using decisions for feedback, which translates into a “threshold behavior” of channel capacity via Lemma 1, cf. Fig. 9. On the other hand, for moderately distorting channels like the dicode (Fig. 7), a smooth transition occurs in the capacity curve.

Finally, the results for MMSE-LE (dash-dotted lines, “×”) indicate that optimum soft-output equalization and Wiener filtering are equivalent for low signal-to-noise ratios. This holds because binary and Gaussian input signals cannot be distinguished in this regime and the Wiener filter is the optimum detector for Gaussian symbols. on and decoding (“*”) and

V. SUMMARY AND CONCLUSION

The problem of separate detection and decoding was tackled introducing an equivalent binary-symmetric channel with varying crossover probability. Results were provided for two examples: CDMA and ISI. In these two examples, the capacity of separate detection and decoding was found to be far behind the capacity of joint decoding for high interference levels. This suggests that in many cases, the prohibitive complexity of joint decoding can only be overcome by iterative decoding methods or, alternatively, MMSE-DFE which comes surprisingly close to channel capacity also for binary signals, cf. also [27].

APPENDIX I PROOF OF LEMMA 1

Let the channel input be denoted without loss of generality by $X \in \{0; 1\}$. Thus, we find

$$I(X; Y) = H(X) - H(X|Y) \quad (28)$$

$$= H(X) - \mathbb{E}_y H(X|Y = y) \quad (29)$$

$$= H(X) + \sum_{i=0}^1 \mathbb{E}_y \left[\Pr(X = i|Y = y) \times \log_2 \Pr(X = i|Y = y) \right] \quad (30)$$

$$= H(X) - \mathbb{E}_y \mathcal{H}(\Pr(X = 1|Y = y)) \quad (31)$$

$$= H(X) - \mathbb{E}_y \mathcal{H}(\Pr(X = 0|Y = y)). \quad (32)$$

Now, assume that $X = 0$ was sent. Then, $\Pr(X = 1|Y = y)$ is the probability of error and (31) proves the lemma. Alternatively, assume that $X = 1$ was sent. Then, $\Pr(X = 0|Y = y)$ is the probability of error and (32) proves the lemma. Since there are no other choices for X , the proof is complete. \square

APPENDIX II FIRST PROOF OF PROPOSITION 2

From [4, eq. (47)], we have in the large system limit for any analytic function $f(\cdot)$

$$\mathbb{E}_r f[1 - 2P_e(p_1)] = \sqrt{\frac{\eta}{2\pi\sigma^2}} \int_{\mathbb{R}} f \left[\tanh\left(\frac{\eta}{\sigma^2}x\right) \right] \times \exp\left(-\frac{\eta(x-1)^2}{2\sigma^2}\right) dx. \quad (33)$$

Choosing $f(x) = \mathcal{H}\left(\frac{1}{2} - \frac{1}{2}x\right)$, we find with Lemma 1

$$C_{\text{sep}} = 1 - \sqrt{\frac{\eta}{2\pi\sigma^2}} \int_{\mathbb{R}} \mathcal{H}\left[\frac{1}{2} - \frac{1}{2} \tanh\left(\frac{\eta}{\sigma^2}x\right)\right] \times \exp\left(-\frac{\eta(x-1)^2}{2\sigma^2}\right) dx \quad [\text{bit}]. \quad (34)$$

Note that

$$1 - \mathcal{H}\left[\frac{1}{2} - \frac{1}{2} \tanh(x)\right] = 1 - \mathcal{H}\left[\frac{e^{-x}}{e^x + e^{-x}}\right] \quad (35)$$

$$= 1 - \frac{e^{-x}}{e^x + e^{-x}} \log_2\left(\frac{e^x + e^{-x}}{e^{-x}}\right) - \frac{e^x}{e^x + e^{-x}} \log_2\left(\frac{e^x + e^{-x}}{e^x}\right) \quad (36)$$

$$= 1 - \log_2(e^x + e^{-x}) + \frac{x}{\ln 2} \cdot \frac{e^x - e^{-x}}{e^x + e^{-x}} = -\log_2[\cosh(x)] + \frac{x \tanh(x)}{\ln 2}. \quad (37)$$

Moreover, consider the general problem of nonlinear MMSE estimation of binary signals in Gaussian noise. Note that the nonlinear MMSE estimate is given by $\tanh(\alpha x)$ where x is the (normalized) input signal of the estimator and α is the signal-to-noise ratio. Conditioned on the transmission of $+1$, the estimation error is $1 - \tanh(\alpha x)$. Since the estimation error is orthogonal to the signal x , we find

$$\int_{\mathbb{R}} x [1 - \tanh(\alpha x)] \exp\left(-\frac{\alpha}{2}(x-1)^2\right) dx = 0 \quad (38)$$

$\forall \alpha > 0$ yielding

$$\sqrt{\frac{\alpha}{2\pi}} \int_{\mathbb{R}} \alpha x \tanh(\alpha x) \exp\left(-\frac{\alpha}{2}(x-1)^2\right) dx = \alpha \quad (39)$$

$\forall \alpha > 0$.

Combining (34), (37), and (39), the proof is complete. \square

APPENDIX III SECOND PROOF OF PROPOSITION 2

The chain rule of mutual information [40] states

$$I(X_1, \dots, X_K; \mathbf{R}) = \sum_{k=1}^K I(X_k; \mathbf{R}|X_{k+1}, \dots, X_K). \quad (40)$$

Note that $kI(X_k; \mathbf{R}|X_{k+1}, \dots, X_K)$ is the capacity for separate decoding in presence of k users, since known additive interference does not affect mutual information. Defining $\beta' = k/N$, we find in the large system limit (by the definition of the Riemann integral and in analogy to [11, eq. (100)])

$$C_{\text{joint}} = \frac{1}{\beta} \int_0^\beta C_{\text{sep}}(\beta') d\beta'. \quad (41)$$

Defining

$$S \triangleq C_{\text{joint}} - \frac{\eta - 1 - \log \eta}{2\beta} \quad (42)$$

and solving for C_{sep} yields

$$C_{\text{sep}} = \frac{d}{d\beta} (\beta C_{\text{joint}}) \quad (43)$$

$$= \frac{d}{d\beta} \left(\beta S + \frac{\eta - 1 - \log \eta}{2} \right) \quad (44)$$

$$= S + \beta \frac{d}{d\beta} S + \frac{d}{d\beta} \frac{\eta - \log \eta}{2} \quad (45)$$

$$= S + \left(\frac{1}{2} - \frac{1}{2\eta} + \beta \frac{d}{d\eta} S \right) \frac{d\eta}{d\beta}. \quad (46)$$

Since we want to show that $C_{\text{sep}} = S$, we must prove the bracketed expression in (46) to vanish. We find

$$\beta \frac{d}{d\eta} S = \frac{\beta}{\sigma^2} - \frac{\beta}{\sqrt{2\pi}} \frac{d}{d\eta} \int_{\mathbb{R}} \exp\left(-\frac{x^2}{2}\right) \times \log \cosh\left(\sqrt{\frac{\eta}{\sigma^2}}x + \frac{\eta}{\sigma^2}\right) dx \quad (47)$$

$$= \frac{\beta}{\sigma^2} - \frac{\beta}{\sqrt{2\pi\sigma^2}} \int_{\mathbb{R}} \tanh\left(\sqrt{\frac{\eta}{\sigma^2}}x + \frac{\eta}{\sigma^2}\right) \times \left(1 + \frac{x}{2\sqrt{\eta/\sigma^2}}\right) \exp\left(-\frac{x^2}{2}\right) dx \quad (48)$$

$$= \frac{\beta}{\sigma^2} - \frac{\beta}{2\sigma^2} \sqrt{\frac{\eta}{2\pi\sigma^2}} \int_{\mathbb{R}} \tanh\left(\frac{\eta}{\sigma^2}x\right) \times (x+1) \exp\left(-\frac{\eta(x-1)^2}{2\sigma^2}\right) dx \quad (49)$$

$$= \frac{\beta}{2\sigma^2} - \frac{\beta}{2\sigma^2} \sqrt{\frac{\eta}{2\pi\sigma^2}} \int_{\mathbb{R}} \tanh\left(\frac{\eta}{\sigma^2}x\right) \times \exp\left(-\frac{\eta(x-1)^2}{2\sigma^2}\right) dx \quad (50)$$

$$= \frac{1}{2\eta} - \frac{1}{2} \quad (51)$$

where (50) and (51) follow from (39) and (12), respectively. \square

APPENDIX IV

THIRD (HEURISTIC) PROOF OF PROPOSITION 2

This proof requires an additional assumption in comparison to the previous two proofs and is therefore less rigorous. However, it gives additional insight into the problem due to the formulation of an equivalent AWGN channel.

According to [4, Lemma 1], the m th moment of the soft output of the individually optimum multiuser detector obtained by averaging over all interfering users, signature sequences, and noise is given in the large system limit by

$$\sqrt{\frac{\eta}{2\pi\sigma^2}} \int_{\mathbb{R}} \tanh^m\left(\frac{\eta}{\sigma^2}x\right) \exp\left(-\frac{\eta(x-1)^2}{2\sigma^2}\right) dx. \quad (52)$$

For this, it has been assumed that the multiuser detector delivers the a posteriori expectation (nonlinear MMSE estimate) of the transmitted symbols and that the user of interest transmits $x_k = 1$.

The moments of the soft output of a binary-input AWGN channel with signal-to-noise ratio $\alpha = \eta/\sigma^2$ are given by (52), as well (see Appendix II). Hence, if the self-averaging property with respect to the signature sequences holds for all moments, i.e., they converge in the large system limit,¹² the overall channel seen by the decoder is statistically equivalent to a binary-input AWGN channel with signal-to-noise ratio $\alpha = \eta/\sigma^2$. The fact that this equivalent channel is an AWGN channel has also been found independently in a recent work of Guo and Verdú [12].

It is straightforward to calculate mutual information for this equivalent channel. Let the noise variance of the equivalent AWGN channel be σ^2/η and define the pdf

$$f_m(x) = \sqrt{\frac{\eta}{8\pi\sigma^2}} \left[\exp\left(-\frac{\eta}{2\sigma^2}(x-1)^2\right) + \exp\left(-\frac{\eta}{2\sigma^2}(x+1)^2\right) \right] \quad (53)$$

¹²This is the additional assumption which is not required in the first proof. Note that in the first proof, it is enough to *average* over the signature sequences due to Lemma 1.

$$= \sqrt{\frac{\eta}{2\pi\sigma^2}} \exp\left(-\frac{\eta}{2\sigma^2}(x^2+1)\right) \times \cosh\left(\frac{\eta}{\sigma^2}x\right) \quad (54)$$

(index “ m ” stands for Gaussian mixture). Then, we find for the capacity with separate detection and decoding

$$C_{\text{sep}} = I(X; P_1) \quad (55)$$

$$= I(X; \text{artanh}(2P_1 - 1)) \quad (56)$$

$$= h(\text{artanh}(2P_1 - 1)) - h(\text{artanh}(2P_1 - 1)|X_1) \quad (57)$$

$$= - \int_{\mathbb{R}} f_m(x) \log f_m(x) dx - \frac{1}{2} \log(2\pi\epsilon\sigma^2/\eta) \quad (58)$$

$$= \int_{\mathbb{R}} f_m(x) \left[\frac{\eta}{2\sigma^2}(x^2+1) - \log \cosh\left(\frac{\eta}{\sigma^2}x\right) \right] dx - \frac{1}{2} \quad (59)$$

$$= \frac{\eta}{2\sigma^2} \left(\frac{\sigma^2}{\eta} + 1 + 1 \right) \quad (60)$$

$$- \int_{\mathbb{R}} f_m(x) \log \cosh\left(\frac{\eta}{\sigma^2}x\right) dx - \frac{1}{2}$$

$$= \frac{\eta}{\sigma^2} - \sqrt{\frac{\eta}{2\pi\sigma^2}} \int_{\mathbb{R}} \log \left[\cosh\left(\frac{\eta}{\sigma^2}x\right) \right]$$

$$\times \exp\left(-\frac{\eta(x-1)^2}{2\sigma^2}\right) dx \quad [\text{nat}]. \quad (61)$$

This completes the proof. \square

ACKNOWLEDGMENT

The authors would like to thank Jossy Sayir and the anonymous reviewers for their very helpful comments.

REFERENCES

- [1] S. Shamai (Shitz) and S. Verdú, “The impact of frequency-flat fading on the spectral efficiency of CDMA,” *IEEE Trans. Inform. Theory*, vol. 47, pp. 1302–1327, May 2001.
- [2] ETSI, “GSM Specifications,” Series 01-12, 1991.
- [3] L. Bahl, J. Cocke, F. Jelinek, and J. Raviv, “Optimal decoding of linear codes for minimizing symbol error rate,” *IEEE Trans. Inform. Theory*, vol. IT-20, pp. 284–287, Mar. 1974.
- [4] T. Tanaka, “A statistical mechanics approach to large-system analysis of CDMA multiuser detectors,” *IEEE Trans. Inform. Theory*, vol. 48, pp. 2888–2910, Nov. 2002.
- [5] S. Verdú, “Minimum probability of error for asynchronous Gaussian multiple-access channels,” *IEEE Trans. Inform. Theory*, vol. IT-32, pp. 85–96, Jan. 1986.
- [6] S.-Y. Chung, “On the construction of some capacity-approaching coding schemes,” Ph.D. dissertation, MIT, Cambridge, MA, 2000.
- [7] R. R. Müller, “Combining multiuser detection with coding: Promises and problems,” in *Proc. Conf. Information Science and Systems (CISS)*, Princeton, NJ, Mar. 2000, pp. WA3-17–WA3-22.
- [8] H. Nishimori, *Statistical Physics of Spin Glasses and Information Processing*. Oxford, U.K.: Oxford Univ. Press, 2001.
- [9] —, “Comment on statistical mechanics of CDMA multiuser demodulation by T. Tanaka,” *Europhys. Lett.*, vol. 57, no. 2, pp. 302–303, Jan. 2002.
- [10] S. Verdú, *Multiuser Detection*. New York: Cambridge Univ. Press, 1998.
- [11] S. Verdú and S. Shamai (Shitz), “Spectral efficiency of CDMA with random spreading,” *IEEE Trans. Inform. Theory*, vol. 45, pp. 622–640, Mar. 1999.
- [12] D. Guo and S. Verdú, “Multiuser detection and statistical mechanics,” in *Communications, Information and Network Security*, V. Bhargava, H. V. Poor, V. Tarokh, and S. Yoon, Eds. Norwell, MA: Kluwer Academic, 2002, pp. 229–278.
- [13] R. R. Müller, “On channel capacity, uncoded error probability, ML-detection, and spin glasses,” in *Proc. Workshop on Concepts in Information Theory*, Breisach, Germany, June 2002, pp. 79–81.
- [14] D. Guo and S. Verdú, “Replica analysis of large-system CDMA,” in *Proc. IEEE Information Theory Workshop (ITW)*, Paris, France, Mar./Apr. 2003.

- [15] —, “CDMA spectral efficiency: Asymptotics via statistical physics,” *IEEE Trans. Inform. Theory*, submitted for publication.
- [16] D. N. C. Tse and S. Hanly, “Linear multiuser receivers: Effective interference, effective bandwidth and user capacity,” *IEEE Trans. Inform. Theory*, vol. 45, pp. 641–657, Mar. 1999.
- [17] H. V. Poor and S. Verdú, “Probability of error in MMSE multiuser detection,” *IEEE Trans. Inform. Theory*, vol. 43, pp. 858–871, May 1997.
- [18] J. Zhang, E. K. Chong, and D. N. C. Tse, “Output MAI distributions of linear MMSE multiuser receivers in DS-CDMA systems,” *IEEE Trans. Inform. Theory*, vol. 47, pp. 1128–1144, Mar. 2001.
- [19] R. R. Müller, *Power and Bandwidth Efficiency of Multiuser Systems with Random Spreading*. Aachen, Germany: Shaker-Verlag, 1999.
- [20] D. N. C. Tse and S. Verdú, “Optimum asymptotic multiuser efficiency of randomly spread CDMA,” *IEEE Trans. Inform. Theory*, vol. 46, pp. 2718–2722, Nov. 2000.
- [21] A. J. Viterbi and J. K. Omura, *Principles of Digital Communications and Coding*. Tokyo, Japan: McGraw-Hill, 1979.
- [22] M. K. Varanasi and T. Guess, “Optimum decision feedback multiuser equalization with successive decoding achieves the total capacity of the Gaussian multiple-access channel,” in *Proc. Asilomar Conf. Signals, Systems and Computers*, Monterey, CA, Nov. 1997, pp. 1405–1409.
- [23] W. Koch and A. Baier, “Optimum and sub-optimum detection of coded data disturbed by time-varying intersymbol interference (applicable to digital mobile radio receivers),” in *Proc. IEEE Global Telecommunication Conf. (GLOBECOM)*, San Diego, CA, Dec. 1990, pp. 1679–1684.
- [24] R. G. Gallager, *Information Theory and Reliable Communication*. New York: Wiley, 1968.
- [25] H. Pfister, J. Soriaga, and P. H. Siegel, “On the achievable information rates of finite state ISI channels,” in *Proc. IEEE Global Telecommunications Conf. (GLOBECOM’01)*, San Antonio, TX, Nov. 2001, pp. 2992–2996.
- [26] A. Kavčić, X. Ma, and M. Mitzenmacher, “Binary intersymbol interference channels: Gallager codes, density evolution, and code performance bounds,” *IEEE Trans. Inform. Theory*, vol. 49, pp. 1636–1652, July 2003.
- [27] S. Shamai (Shitz) and R. Laroia, “The intersymbol interference channel: Lower bounds on capacity and channel precoding loss,” *IEEE Trans. Inform. Theory*, vol. 42, pp. 1388–1404, Sept. 1996.
- [28] D. Arnold and H.-A. Loeliger, “On the information rate of binary-input channels with memory,” in *Proc. IEEE Int. Conf. Communications (ICC)*, Helsinki, Finland, June 2001, pp. 2692–2695.
- [29] V. Sharma and S. Singh, “Entropy and channel capacity in the regenerative setup with applications to Markov channels,” in *Proc. Int. Symp. Information Theory (ISIT 2001)*, Washington, D.C., June 2001, p. 283.
- [30] A. Kavčić, “On the capacity of Markov sources over noisy channels,” in *Proc. IEEE Global Telecommunications Conf. (Globecom’01)*, San Antonio, TX, Nov. 2001, pp. 2997–3001.
- [31] S. Yang, A. Kavčić, and S. Tatikonda, “Delayed feedback capacity of finite-state machine channels: Upper bounds on the feedforward capacity,” in *Proc. Int. Symp. Information Theory (ISIT’03)*, Yokohama, Japan, June/July 2003, p. 290.
- [32] J. Cioffi, G. Dudevoir, M. Eyuboglu, and G. D. Forney Jr, “MMSE decision-feedback equalizers and coding—Parts I and II,” *IEEE Trans. Commun.*, vol. 43, pp. 2582–2604, Oct. 1995.
- [33] J. G. Proakis, *Digital Communications*, 3rd ed. New York: McGraw-Hill, 1995.
- [34] R. Price, “Nonlinear feedback equalized PAM versus capacity for noisy filter channels,” in *Proc. IEEE Int. Conf. Communications (ICC)*, Philadelphia, PA, June 1972, pp. 22.12–22.17.
- [35] T. Guess and M. Varanasi, “A new successively decodable coding technique for intersymbol-interference channels,” in *Proc. IEEE Int. Symp. Information Theory (ISIT’00)*, Sorrento, Italy, June 2000, p. 102.
- [36] R. Zamir, S. Shamai (Shitz), and U. Erez, “Nested linear/lattice codes for structured multiterminal binning,” *IEEE Trans. Inform. Theory*, vol. 48, pp. 1250–1276, June 2002.
- [37] M. Tomlinson, “New automatic equaliser employing modulo arithmetic,” *IEE Electron. Lett.*, vol. 7, pp. 138–139, Mar. 1971.
- [38] H. W. Schübler, *Digitale Signalverarbeitung 1*, 4th ed. Berlin, Germany: Springer-Verlag, 1994.
- [39] A. Rony and S. Shamai (Shitz), “Suboptimal detection for intersymbol interference inflicted cable channels,” *Int. J. Electron. Commun. (AEÜ)*, vol. 51, no. 5, pp. 246–254, 1997.
- [40] T. M. Cover and J. A. Thomas, *Elements of Information Theory*. New York: Wiley, 1991.

On Skew Information

Shunlong Luo and Qiang Zhang

Abstract—We show that skew information introduced by Wigner and Yanase, which is a natural informational extension of variance for pure states, can be interpreted as a measure of quantum uncertainty. By virtue of skew information, we establish a new uncertainty relation in the spirit of Schrödinger, which incorporates both incompatibility (encoded in the commutator) and correlations (encoded in a new correlation measure related to skew information) between observables, and moreover is stronger than the conventional ones.

Index Terms—Fisher information, quantum estimation, quantum states, skew information, uncertainty relations.

I. INTRODUCTION

In their study of quantum measurement theory and information contents of quantum states (mixed states, density operators), Wigner and Yanase [30] introduced the quantity

$$I(\rho, H) := -\frac{1}{2}\mathrm{tr}[\rho^{1/2}, H]^2$$

which they called skew information to express the amount of information on the values of observables *not* commuting with H (tr denotes trace and the square bracket denotes commutator). Here H is interpreted as a conserved quantity, such as a Hamiltonian or a momentum, of the relevant quantum system. Wigner and Yanase argued and proved that this quantity satisfies a variety of desirable intuitive requirements for an information-theoretic measure, among which the basic ones are as follows: 1) Skew information remains constant for isolated systems, thus, I is invariant as long as the state changes according to the Landau-von Neumann. 2) Skew information decreases when two different ensembles are united, since by uniting, one “forgets” from which ensemble a particular sample stems. 3) Skew information is additive, namely, the information content of a system composed of two independent parts is the sum of information of the parts.

More than 40 years have passed since skew information was introduced in 1963. To the best of our knowledge, almost no one has ever made explicit use of this concept in the theory of quantum measurement, although the mathematical characterizations and properties of skew information have been studied extensively by some authors, notably, Gibilisco and Isola [8]–[10], Grasselli [11], Hasegawa *et al.* [12]–[16], Jencová [20], [21], Petz *et al.* [24]–[27], among others. In these works, skew information is interpreted as a kind of quantum Fisher information from a geometric perspective. An interesting and singular application of skew information in solving mathematical problems is [5], in which Connes and Stormer have made use of it in proving the homogeneity of state spaces of type III₁ von Neumann algebras.

Manuscript received November 4, 2003; revised February 8, 2004. The work of S. Luo was supported by the National Science Foundation of China under Grant 10131040. The work of Q. Zhang was supported in part by the Research Grants Council of Hong Kong, Project CityU 1221/02P.

S. Luo is with the School of Mathematics and Statistics, Carleton University, Ottawa ON K1S 5B6, Canada, on leave from the Academy of Mathematics and Systems Sciences, Chinese Academy of Sciences, 100080 Beijing, China (e-mail: luosl@mail.amt.ac.cn).

Q. Zhang is with the Department of Mathematics, City University of Hong Kong, Kowloon, Hong Kong (e-mail: mazq@math.cityu.hk).

Communicated by E. H. Knill, Associate Editor for Quantum Information Theory.

Digital Object Identifier 10.1109/TIT.2004.831853